The Journal of Physical Chemistry A

 VOLUME 102, NUMBER 4, JANUARY 22, 1998

LETTERS

Femtosecond Dynamics of a Hydrogen-Bonded Model Base Pair in the Condensed Phase: Double Proton Transfer in 7-Azaindole

M. Chachisvilis,[†] T. Fiebig,[‡] A. Douhal,[§] and A. H. Zewail*

Arthur Amos Noyes Laboratory of Chemical Physics, California Institute of Technology, Pasadena, California 91125

Received: November 25, 1997; In Final Form: December 10, 1997

Femtosecond, real-time dynamics of a hydrogen-bonded model base pair (7-azaindole dimer) in the condensed phase is presented and compared with gas-phase, molecular beam studies. Following the preparation of a wave packet (nonequilibrium state), we resolved the initial decay of the reactive pair and the rise of the tautomer in two solvents. Studies of the isotope effect, solvent viscosity, energy dependence, and polarization anisotropy are consistent with direct and indirect reaction pathways for the double proton transfer on a global potential energy surface.

I. Introduction

The dynamics of proton transfer in hydrogen-bonded systems is central to the understanding of many phenomena.[1,2] One class of molecules of great interest is that mimicking the behavior of a base pair and where double proton transfer can take place. In the prototype system of 7-azaindole (Figure 1), it was discovered that its dimer exhibits the phenomenon of double proton transfer upon excitation by a UV photon.[3] Since then much work in the condensed phase has been reported with the goal of understanding the effect of solvation (see, e.g., refs 4−6), the catalytic transfer with external solvents,[7] and the energetics and equilibrium properties of the spectra.[8,9] The first picosecond study[10] showed that this transfer occurs in less than 5 picosecond (ps), and subpicosecond resolution[11] indicated that the time constant is 1.4 ps. In the latter study,[11] it was suggested that another channel, forming the ground-state tautomer, is operative on the same time scale of the laser pulse width.

The dynamics of the *isolated* base-pair structure is key to understanding the mechanism, given that the complexity of the interaction with the solvent may lead to intramolecular vibrational-energy redistribution (IVR) and to vibrational relaxation (VR) on the time scale of the transfer. Douhal et al.[12] reported studies of the femtosecond (fs) dynamics of the isolated pair in a molecular beam using time-resolved mass spectrometry. The results showed the dependence of rates on the total (vibrational) energy with a large (factor of 10) isotope effect on the observed biexponential decay. Even near the zero-point energy, the transfer was observed: $E \sim 0$ cm^{-1} ($\tau_1 = 650$ fs, $\tau_2 = 3.3$ ps); $E \sim 500$ cm^{-1} ($\tau_1 = 200$ fs, $\tau_2 = 1.6$ ps). It was concluded that a global potential energy surface (PES), involving at least the N−H and N···N vibrational motions, describes the non-concerted pathway for the transfer and that tunneling is significant. Theoretical calculations[13] of the reaction path confirmed this picture. Furthermore, photoelectron spectral study[14] with subpicosecond resolution is consistent with the time scale of the transfer. Recently, using Coulomb explosion techniques, it was demonstrated elegantly by the group of Castleman (private communication) that the intermediate can be arrested and that the time scales for its buildup (∼0.7 ps)

[†] Postdoctoral fellowship from the Swedish Foundation for International Cooperation in Research and Higher Education.

[‡] Postdoctoral fellowship from the Deutsche Forschungsgemeinschaft.

[§] Departamento de Química Física, Facultad de Químicas, Sección de Toledo, Universidad de Castilla-La Mancha, San Lucas, 3, 45002, Toledo, Spain.

S1089-5639(98)00337-5 CCC: $15.00
Published on Web 01/06/1998

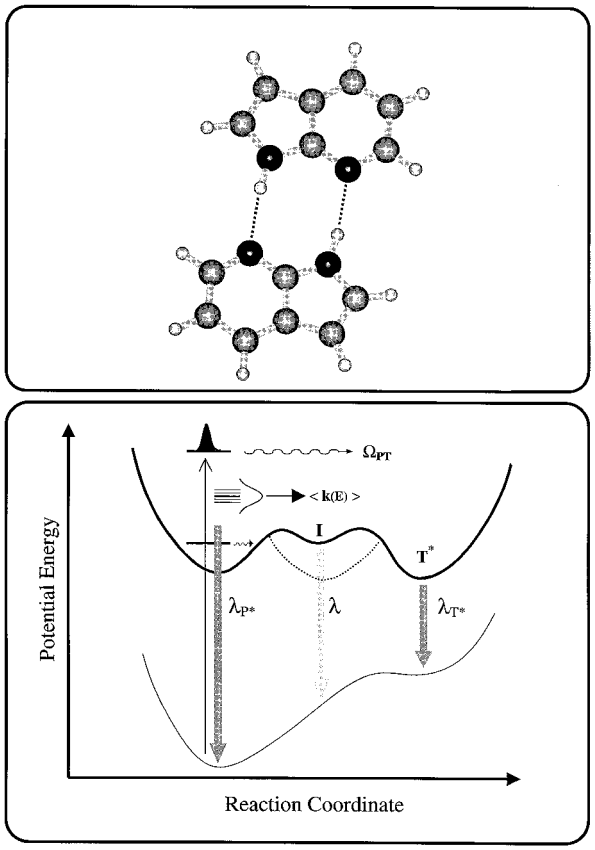

Figure 1. (Top) Structure of the 7-azaindole pair with two hydrogen bonds. (Bottom) A schematic of the potential energy profile corresponding to the double proton transfer reaction. The dotted curve is to indicate the possible influence of the solvent.

and its decay (a few picoseconds) are in agreement with the findings of Douhal et al.[12]

Earlier, the spectrum of the dimer in supersonic jets[15] has shown the vibrational progression of involved modes. The symmetric stretching (N−H···N) vibration of the hydrogen bond promotes the transfer. The bandwidth in the excitation spectra (monitored through the tautomer emission) of the $\upsilon' = 1$ and $\upsilon' = 2$ of this 120-cm^{-1} vibration was found to be ∼10 and 30 cm^{-1}, respectively, inferring lifetimes of ∼0.5 and 0.2 ps. This time scale is consistent with the initial component of the decay.[12] It should be noted, however, that the bands may be inhomogeneously broadened and in fact they display wings which reflect the presence of more than one process. Other spectroscopic studies[16] have addressed the nature of the nonreactive pairs and the complexes with solvents such as water.

In continuation of our efforts, we report in this Letter femtosecond, time-resolved studies of the same pair but now in the solution phase. The transition from the gas phase to the condensed phase helps us in elucidating the role of IVR and VR, the effect of solvent structure and viscosity, and the isotope effect on the dynamics. Using fluorescence upconversion techniques, we resolve the rise of the tautomer population and also the decay of the initial reactive pair. With these studies in two solvents (hexadecane and 3-methylpentane) and by examining the effect of deuterium replacement of protons (of the NH system) and the polarization anisotropy, we establish that the primary transfer of protons in the condensed phase takes 1 ps. We also provide a description of the nature of direct and indirect transfer on the global PES.

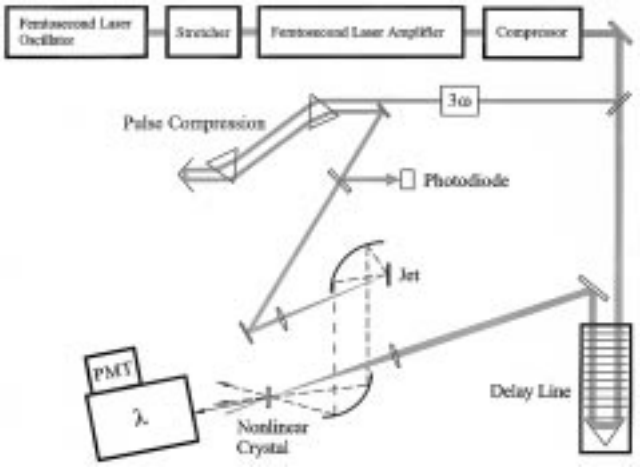

Figure 2. Schematic of the experimental apparatus (see text).

II. Experimental Section

The fluorescence upconversion experiments were performed with a setup that is shown schematically in Figure 2. The system consists of a femtosecond Ti:sapphire oscillator coupled to a regenerative amplifier that generates 90-fs, 0.6-mJ light pulses. The pulses are centered around 798 nm at 1-kHz repetition rate. A beam splitter was used to divide the light beam into the excitation and gating branches with a 4-to-1 ratio. The excitation pulses were tripled to yield 266-nm pulses using two 0.2-mm BBO crystals. These pulses were subsequently compressed, using two silica prisms to compensate for group velocity dispersion, and focused into the sample, which flows through a jet. This arrangement was introduced to minimize the effects of laser-induced photochemistry (we have found out that it is advantageous to use a jet because the photoproducts tend to form a film on the quartz windows of a flow cell which is highly emitting in the region of interest).

Typically the energy of the excitation pulse at the sample was ∼30 nJ. At these energies, the fluorescence signal from our samples was linearly dependent on the excitation intensity. To examine the population dynamics, the polarization of the excitation light was set at the magic angle with respect to that of the gating pulse. We also studied carefully the behavior of the signal in (∥, ∥) and (∥, ⊥) configurations to examine the role of the anisotropy.

The sample fluorescence was collected and focused into a nonlinear crystal (0.2 mm, BBO, type I) using reflective optics. The gating pulse was time delayed and also focused into the nonlinear crystal to overlap with the sample fluorescence. The resulting sum-frequency signal in the UV region was filtered using a double monochromator and detected with a photomultiplier tube. When necessary the signal was also normalized to the energy of the excitation pulse. The temporal response function of the pulses and detection is ∼ 300 fs. Since the pulse width is 90 fs, the resolution is only limited by the detection arrangement.

7-Azaindole (7-AI) (98% purchased from Aldrich Inc.) was purified by vacuum sublimation. Two solvents (both from Aldrich Inc.) were used: anhydrous hexadecane (water < 0.005%) and 3-methylpentane (99+%). N′-deuterated 7-azaindole was prepared by dissolving 7-azaindole in O′-deuterated ethyl alcohol (isotopic purity 99.5%) and keeping the solution at 70 °C for ∼15 min, and subsequent vacuum evaporation. Typically five cycles were performed. The ^{1}H NMR and mass spectral analysis gave isotopic purity of ∼80%.

We have determined that any contact of the solution with a metal surface leads to gradual disintegration of the sample and

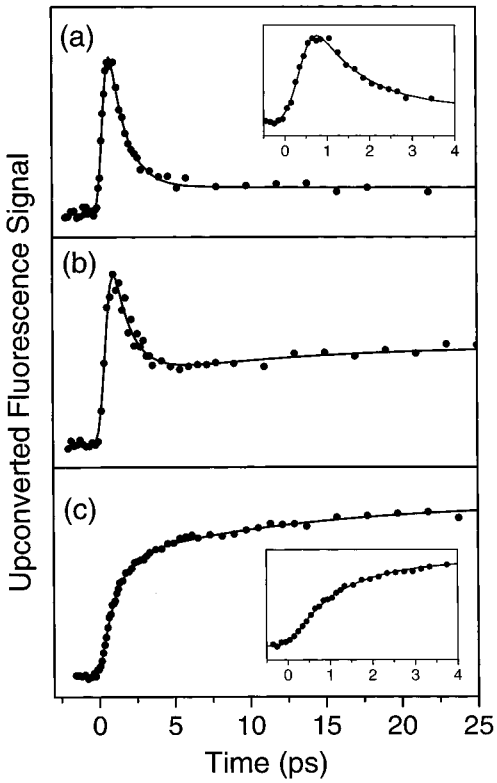

Figure 3. Femotsecond transients of 7-AI in solutions of hexadecane. The emission was gated at (a) 360, (b) 440, and (c) 480 nm. The inserts show an enlargement of the early-time behavior. The excitation was at 266 nm. Other solvents and excitation and fluorescence wavelengths were studied similarly (see text).

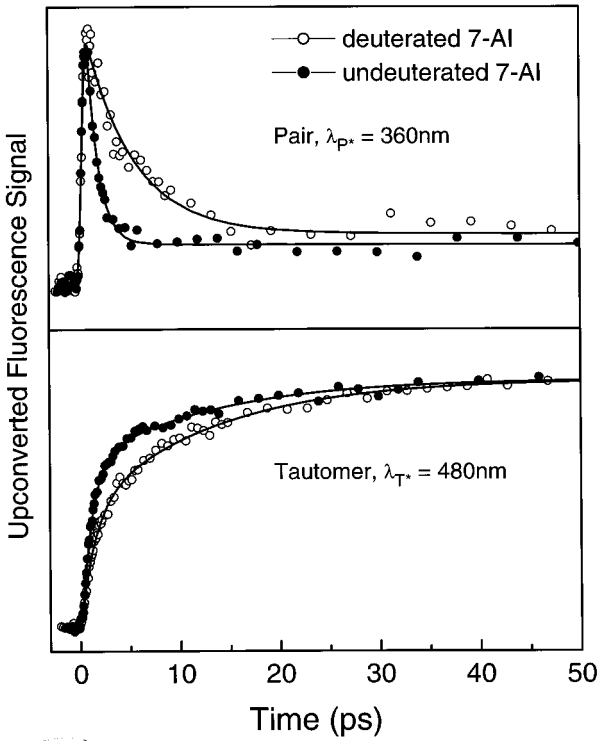

Figure 4. Femtosecond transients of 7-AI in solutions of hexadecane. The emission was gated at (a) 360 and (b) 480 nm. The excitation was at 266 nm. Results for both 7-AI deuterated and undeuterated species are shown.

formation of other strongly fluorescing species. Therefore, all parts of the jet system were made of Teflon and glass. Additionally, to protect the sample from atmospheric moisture, the experiments were carried out in a dry argon atmosphere. The laser excitation of the solvent alone did not produce any signal that we could detect. Besides the steady-state fluorescence and excitation spectra, the purity of 7-AI was checked by mass spectrometry and high-performance liquid chromatography (HPLC); no evidence of impurity was found.

III. Results and Discussion

With CW UV excitation, 7-azaindole (7-AI) displays a broad emission band ranging from 420 to about 600 nm in nonpolar solvents.[3,4] This band has a maximum at 480 nm. In our samples, we have observed this characteristic emission spectra and also the excitation spectra. The 480-nm band has been shown to arise from the tautomer (T*) after proton transfer; 7-AI tautomer and 7-methyl-7*H*-pyrrole[2,3-6]pyridine display very similar emission spectra.[4] Additionally, there is a second band, extending from 290 nm and up to 430 nm, which is due to the emission of 7-AI monomer and dimer. For CW excitation, the dimer emission occurs around 360 nm. This is based on our experiments with excitations at 266 versus 320 nm. For the latter, we observed much weaker emission, than for the monomer, and this emission is shifted to 360 nm in contrast with the monomer emission at 320 nm. This result is consistent with those of previous work obtained at 200 K or lower.[4]

The femtosecond-resolved fluorescence transients were obtained at the emission bands corresponding to the dimer and the tautomer, namely, at 360 and 480 nm. We also studied the emission at 440, 460, 500, and 520 nm. Figure 3 shows transients of 7-AI dissolved in hexadecane at three different wavelengths. At 360 nm (Figure 3a), we obtained a decay with a 1-ps time constant. At 480 nm, we observed a biexponential rise (Figure 3c). The short-time component of the rise is ~1 ps, and the long-time component is ~12 ps. When the detection was at 440 nm, the observed transient can be considered as a superposition of dimer and tautomer contributions. We note that even though the quantum yield of the dimer fluorescence (steady state) is reduced considerably because of proton transfer, at short times there is enough population to observe the change in population with time.

To investigate the role of solvent−solute interactions, we carried out experiments in two intrinsically different nonpolar solvents, hexadecane and 3-methylpentane. The femtosecond transients were identical in both solvents, within the accuracy of our experiment. Because the viscosity of the two solvents are different (η = 3.34 cP for hexadecane and $\eta \approx$ 0.3 cP for 3-methylpentane at 20 °C), this behavior indicates the insensitivity of the observed dynamics to solvent structure and viscosity in this range.

The effect of isotopic substitution on the observed transients was also studied. The deuterated 7-AI (*d*-7-AI) was investigated under the same conditions. A comparison of the transient behavior at two different wavelengths is made in Figure 4. It is remarkable that the decay of the dimer fluorescence is substantially influenced by the deuteration: the time constant changes from 1 to 4.5 ps. In contrast, the rise of the tautomer fluorescence shows much less of a change: as shown in Figure 4, the 1-ps component changes to 1.4 ps upon deuteration, whereas no significant change in the 12-ps time constant could be observed. However, the amplitude ratio of the two components is different: for 7-AI the contribution of the short time component is ~65%, whereas for *d*-7-AI a value of ~45% was found.

To test the effect of energy content, we varied the excitation wavelength. The transient fluorescence at 480 nm was detected for three different excitation wavelengths: 266, 306, and 314 nm. For the 306-nm excitation, the 1-ps decay constant increases to 1.6 ps, while the 12-ps component remains similar. Also, the amplitude ratio of the short-time component increases to ~85%. In the case of excitation at 314 nm the overall signal was significantly smaller than that obtained with excitation at 306 nm because of the decrease in absorption. However, we did not observe major changes.

As a further test of the origin of the 12-ps component in the rise, we studied the polarization anisotropy of the rise of the tautomer. For pump-gate (||, ||) arrangement, we observed an additional decay of several hundred ps while for the (||, ⊥) arrangement, this decay component appeared as a rise. These results indicate that the coherent anisotropy decay occurs on a much longer time (65 ps) than the observed population rise (12 ps) at the magic angle (54.7°).

Armed by the finding of gas-phase, isolated pair femtoseconds dynamics,[12] the above results suggest the following model for the condensed-phase transfer dynamics. To begin with, we will assume that the excited-state potential energy has a schematic profile shown in Figure 1. This is based on gas-phase ab initio calculations[13] and emphasizes the nonconcerted pathway of the gas-phase dynamics. The barrier height E_a in the excited state of the 7-AI dimer is ~500−700 cm^{-1}.

The initial femtosecond pulse prepares the dimer in a highly nonequilibrated state. The 0−0 transition of the 7-AI dimer is located at 310 nm (gas phase),[15] while the dimer absorption and fluorescence peaks (solution phase) are at 290 and 360 nm, respectively. Consequently, excitation, for example, at 266 nm prepares the system with approximately 5000 cm^{-1} (not including initial internal energy) above the barrier. It is, therefore, expected that IVR and VR will play a significant role in determining the overall transfer rates.

To elucidate the few possible energy transfer pathways to the reactive mode(s), we consider the multidimensional space comprising all N vibrational modes of the 7-AI dimer $|n_1, n_2, ..., n_i, ..., n_N\rangle$, where n_i denotes the vibrational quantum number of the corresponding mode. The initial excitation prepares a superposition state of the highly energetic vibrational states (a multidimensional wave packet). At later times after excitation this packet is transformed, by IVR and VR, to populations in the reactive coordinates and in coordinates other than the reactive ones. Thus, after excitation the very fast IVR and VR will lead to the creation of two quasi-equilibrated distributions, which we name D_1 and D_2.

The D_1 distribution describes the molecules with the quantum number of the reactive mode (n_r) being 0, 1, ... but less than the height of the barrier: $|0, 0, ..., E_a/\hbar\Omega_{PT} > n_r \geq 0, ..., 0\rangle$; n_1, n_2, ... could also have nonzero values. D_2 represents the situation where the reactive mode is not excited: $|n_1, n_2, ..., n_r = 0, ... n_N\rangle$. These states can be considered to be in thermal equilibrium, though this is not a prerequisite. A vibrational progression with a fundamental frequency $\Omega_{PT} \sim 120$ cm^{-1} was observed in the tautomer excitation spectrum.[15] This mode has been assigned to the N−H···N stretch, which is a reactive mode for proton transfer. As mentioned above, the primary proton transfer out of these states takes place in ~0.6−0.2 ps, depending on the occupation number.[12]

We have considered a kinetic model that treats the behavior of population in the reactive and nonreactive coordinates. The results, shown in Figure 5, reproduce consistency with the biexponential rise of the tautomer population and the exponential decay of the initial pair. From the model, the following picture emerges. The initial step after excitation involves IVR/VR in ~200 fs (preliminary analysis of the rise of the 360 nm emission is consistent with this value). The direct reactive population (D_1) proceeds along the reaction coordinate, and for this channel the isotope effect is dramatic. For the dimer initial decay, the time constant changes from 1 to 4.5 ps upon deuteration. On the other hand, the attenuation of this large isotope effect (only ~50%) on the 1-ps rise component suggests the lack of correspondence between the initial decay and the rise of the 1-ps component. Invoking the intermediate with a lifetime of 12 ps (possibly limited by IVR) we obtained consistent results not only for the isotope effect but also for the relative contributions of the 1 and 12-ps components, which are dictated by the absolute values of the rates and not by fitting.

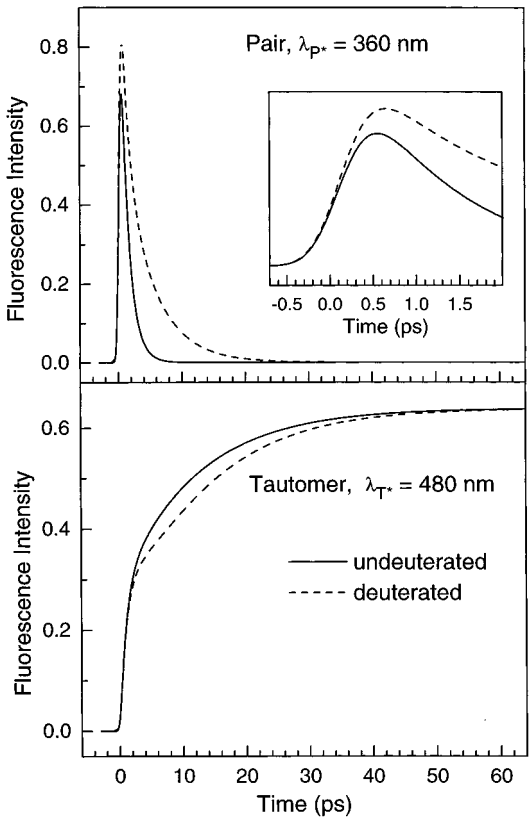

Figure 5. Population dynamics of the initial pair and tautomer excited states for nondeuterated and deuterated species. The calculations were made using a kinetic model for the direct, reactive and indirect population distributions, D_1 and D_2 (see text). The rate constants were derived from the observed transients. Note that there is no long-time residual signal for the 360-nm transient. This is because this offset is primarily due to monomer and some tautomer fluorescence.

At the total available energy of excitation, the indirect transfer of protons involves a thermal (or near thermal) distribution and a barrier of ~ 500 cm^{-1}. This leads to an expected rate of about 10^{13} exp(−500/200), which gives a ~1-ps time constant, consistent with the observed early decay and with being longer than the time for IVR/VR. However, this population does not have the favorable Franck−Condon factor for emission at 360 nm, and the emission is dominated[13] by the direct, reactive population. IVR/VR is presumably similar in the time scale in the tautomer following the transfer. As proposed in ref 10, this population will be trapped upon lowering the temperature and thus lead to a much slower rate.

It is clear that independent of the details of the model the primary transfer occurs in 1 ps, but care has to be taken in

assigning the 12-ps process to a single, secondary process. Besides the nonconcerted pathway, we considered the following possibilities. There could be structural differences of the initial pairs in the solvent; one of them is the reactive one, while another takes time to react. However, this will require the presence of a local energy minimum for a unique structure (not a continuous array of structures) in order to account for only a biexponential rise. The absence of change with solvent viscosity suggests that this possibility is less likely. Moreover, in nonpolar solvents at relatively high concentrations acyclic structures were not detected by NMR spectroscopy.[17] Also some *ground state* tautomers may directly absorb a photon and vibrationally relax or predissociate. However, we found no evidence of tautomer absorption in agreement with results of previous work at 77 K.[18] There could be nearby electronic states that give rise to a different transfer time. We varied the excitation wavelength and did not observe significant changes. Of course, the internal thermal energy of the pair is large, and this explains the robustness of the transients even when the total energy was changed.

In conclusion, the studies presented here for the hydrogen-bonded model base pair (7-AI dimer) in the condensed phase indicate the time scales for double proton transfer and elucidate the role of the solvent on the dynamics of the isolated pair. Isotope effect, solvent structure and viscosity, wavelength tuning, and polarization studies are consistent with the description of direct, reactive and indirect proton transfers. As in the gas-phase work,[12] we believe that the nonconcerted pathway is significant but that on the global PES both trajectories of the symmetric and asymmetric vibrational motions must be considered. Recently, it has also been demonstrated that such pathways are present in a very different system.[19] In the process of writing this work, we learned of a study of dimer excited-state dynamics of 7-AI;[20] the isotope effect and details of the polarization anisotropy were not reported. The lack of the long 12-ps rise in their spectral studies is not understood by us, but it may be that careful extension to longer time scans will show such a component, especially at the 480-nm emission wavelength. Further studies in this laboratory are currently in progress.

Acknowledgment. This work was supported by the National Science Foundation (Laboratory for Molecular Science). M.C. thanks the Swedish Foundation for International Cooperation in Research and Higher Education (STINT) for its generous fellowship. T.F. is grateful for financial support from the Deutsche Forschungsgemeinschaft. A.D. thanks the University of Castilla-La Mancha (Spain) for partial support of his stay at Caltech. We thank Dr. W. Kühnle for his help with HPLC. We also thank the referee for thorough reading of the manuscript and helpful comments.

References and Notes

(1) Schowen, R. L. *Angew. Chem., Int. Ed. Engl*. **1997**, *36*, 1434.
(2) Douhal, A.; Lahmani, F.; Zewail, A. H. *Chem. Phys*. **1996**, *207*, 477 and references therein.
(3) Taylor, C. A.; El-Bayoumi, M. A.; Kasha, M. *Proc. Nat. Acad. Sci. USA* **1969**, *63*, 253.
(4) Ingham, K. C.; El-Bayoumi, M. A. *J. Am. Chem Soc*. **1974**, *96*, 1674.
(5) Smirnov, A. V.; English, D. S.; Rich, R. L.; Lane, J.; Teyton, L.; Schwabacher, A. W.; Luo, S.; Thornburg, R. W.; Petrich, J. W. *J. Phys. Chem. B* **1997**, *101*, 2758.
(6) Chapman, C. F.; Maroncelli, M. *J. Phys. Chem.* **1992**, *96*, 8430.
(7) Chang, C.; Wen-Chen, H.; Meng-Shin, K.; Chou, P.-T.; Clements, J. H. *J. Phys. Chem.* **1994**, *98*, 8801 and references therein.
(8) Tokumura, K.; Watanabe, Y.; Udagawa, M.; Itoh, M. *J. Am. Chem. Soc*. **1987**, *109*, 1346.
(9) Suzuki, T.; Okuyama, U.; Ichimura, T. *J. Phys. Chem. A* **1997,** *101*, 7047 and references therein.
(10) Hetherington, W. M., III; Micheels, R. H.; Eisenthal, K. B. *Chem. Phys. Lett*. **1979**, *66*, 230.
(11) Share, P.; Pereira, M.; Sarisky, M.; Repinec, S.; Hochstrasser, R. M. *J. Lumin.* **1991**, *48/49*, 204.
(12) Douhal, A.; Kim, S. K.; Zewail, A. H. *Nature* **1995**, *378*, 260.
(13) Douhal, A.; Guallar, V.; Moreno, M.; Lluch, J.-M. *Chem. Phys. Lett.* **1996,** *256*, 370.
(14) Lopez-Martens, R.; Long, P.; Solgadi, D.; Soep, B.; Syage, J.; Millie, Ph. *Chem. Phys. Lett*. **1997**, *273*, 219.
(15) Fuke, K.; Kaya, K. *J. Phys. Chem*. **1989**, *93*, 614.
(16) Nakajima, A.; Hirano, M.; Hasumi, R.; Kaya, K.; Watanabe, H.; Carter, C. C.; Williamson, J. M.; Miller, T. A. *J. Phys. Chem. A* **1997,** *101*, 392 and references therein.
(17) Walmsley, J. A. *J. Phys. Chem.* **1981**, *85*, 3181.
(18) Ingham, K. C.; Abu-Elgheit, M.; El-Bayoumi, M. A. *J. Am. Chem. Soc.* **1971**, *93*, 5023.
(19) Marks, D.; Zhang, H.; Glasbeek, M.; Borowicz, P.; Grabowska, A. *Chem. Phys. Lett.* **1997**, *275*, 370.
(20) Takeuchi, S.; Tahara, T. *Chem. Phys. Lett*. **1997**, *277*, 340.